Structure Function Relationships of Estrogenic Triphenylethylenes Related to Endoxifen and 4-Hydroxytamoxifen

Philipp Y. Maximov[1,2], **Cynthia Myers**[1], **Ramona F. Curpan**[3], **Joan S. Lewis-Wambi**[1], and **V. Craig Jordan**[4,*]

[1] Fox Chase Cancer Center, Philadelphia, PA

[2] Russian State Medical University, Moscow, Russia

[3] Institute of Chemistry, Romanian Academy, Timisoara, Romania

[4] Lombardi Comprehensive Cancer Center, Georgetown University, Washington, DC

Abstract

Estrogens can potentially be classified into planar (Class I) or non planar (Class II) categories, which might have biological consequences. 1,1,2-Triphenoplsylethylene (TPE) derivatives were synthesized and evaluated against 17β-estradiol (E2) for their estrogenic activity in MCF-7 human breast cancer cells. All TPEs were estrogenic and unlike 4-hydroxytamoxifen (4OHTAM) and endoxifen, induced cell growth to a level comparable to that of E2. All the TPEs increased ERE activity in MCF-7:WS8 cells with the order of potency as followed: E2 > 1,1-Bis(4,4′-hydroxyphenyl)-2-phenylbut-1-ene (**15**) > 1,1,2-Tris(4-hydroxyphenyl)but-1-ene (**3**) > Z 4-(1-(4-hydroxyphenyl)-1-phenylbut-1-en-2-yl)phenol (**7**) > E 4-(1-(4-hydroxyphenyl)-1-phenylbut-1-en-2-yl)phenol (**6**) > Z(4-(1-(4-ethoxyphenyl)-1-(4-hydroxyphenyl)but-1-en-2-yl)phenol (**12**) > 4-OHTAM. Transient transfection of the ER-negative breast cancer cell line T47D:C4:2 with wild-type ER or D351G ER mutant revealed that all of the TPEs increased ERE activity in the cells expressing the wild-type ER but not the mutant, thus confirming the importance of Asp351 for ER activation by the TPEs. The findings confirm E2 as a Class I estrogen and the TPEs as Class II estrogens. Using available conformations of the ER liganded with 4OHTAM or diethylstilbestrol, the TPEs optimally occupy the 4OHTAM ER conformation that expresses Asp351.

Introduction

Breast cancer is one of the most frequently diagnosed cancers among women in the United States, with an estimated 192,370 new cases of invasive disease and 40,170 deaths in 2009 [1]. Although the exact etiology of breast cancer is not known, there is strong evidence that estrogen plays a role in its development and progression [2]. The effects of estrogen are mediated via the estrogen receptors (ERs), ER-alpha (ERα) and ER-beta (ERβ), which are present in more than eighty percent of breast tumors. With regard to the therapy of breast cancer, ERα remains the most important target and its presence in breast tumors is routinely used to predict response to selective ER modulators (SERMs), such as tamoxifen (TAM) [3, 4]. TAM (Figure 1) is also the first chemotherapeutic drug to target ER-positive breast cancer cells [5] and prevent tumorigenesis in high risk women [6]. TAM is available world wide to treat patients with ER-positive breast cancers.

*To whom correspondence should be addressed: Georgetown University, Lombardi Comprehensive Cancer Center, 3970 Reservoir Rd. NW, Research Bldg., E501, Washington, DC 20057-1468. Telephone: (202) 687-2795. Fax:(202) 687-6402. vcj2@georgetown.edu.

TAM is a substituted derivative [7, 8] of the long acting estrogen triphenylethylene [9]. TAM efficacy depends on the formation of clinically active metabolites 4-hydroxytamoxifen (4OHTAM) [10] and endoxifen [11] (Figure 1) which have a greater affinity to ERα and a much higher antiestrogenic potency in breast cancer cells compared to the parent drug.

We are unaware of the subtle molecular changes that occur when estrogen binds to the ER to produce the ER complex, because the whole complex has not been crystallized. As a consequence of this gap in our knowledge, the modulation of ERα can only be deduced by exploring structure function relationships. However, the Ligand Binding Domain (LBD) of ERα has been crystallized [12, 13] with the estrogens 17β-estradiol (E2), diethylstilbestrol (DES) and the SERMs, 4OHTAM and raloxifene (Figure 1). The resolution of the structure of the estrogen: LBD complex by X-ray crystallography demonstrates that the planar estrogens E2 and DES are sealed within the LBD by helix 12 [12, 13]. This activates Activating Function (AF)-2 at the upper surface of helix 12 by the interaction with coactivators to facilitate full estrogen action. In contrast, the bulky side chain of 4OHTAM and raloxifene prevents helix-12 from sealing the LBD and this produces anti-estrogenic action [12, 13]. However, although AF-2 is deactivated, the 4OHTAM:ERα complex has estrogen-like activity [14], whereas raloxifene does not [15]. This is believed to be because the side chain of raloxifene shields and neutralizes asp351 to block estrogen action [16]. In contrast the side chain of tamoxifen is too short. It appears that when helix 12 is not positioned correctly the exposed asp351 can interact with AF-1 to produce estrogen action. This estrogen-like activity can be inhibited by substituting asp351 for glycine an uncharged amino acid [17].

Planar or non-planar compounds are both classified as estrogens based on their actions to cause growth of the immature rodent uterus or provoke vaginal cornification in castrate animals. However, knowledge of the structure of the 4OHTAM: ER LBD complex [13] led to the idea that all estrogens may not be the same in their interactions with ER [18]. Previous studies suggest that non-planar triphenylethylenes (TPEs) with a bulky phenyl substituent prevents helix-12 from completely sealing the LBD pocket [18]. This physical event creates a putative 'anti-estrogen like' configuration within the complex. However, the complex is not anti-estrogenic because Asp351 is exposed to communicate with AF-1 thereby causing estrogen-like action. Thus, there are putative Class I (planar) and Class II (non-planar) estrogens [18]. A similar classification and conclusion has been proposed [19], but the biological consequences of this classification are unknown.

In this report we further addressed the hypothesis that the shape of the ER complex can be controlled by the shape of an estrogen. We have synthesized a range of hydroxylated TPEs to establish new tools to investigate the relationship of shape with estrogenic activity through the exposure of Asp351. For convenience, the structure of nonsteroidal antiestrogens described in the text are illustrated in Figure 1 and the test compounds in Table 1.

Results

Chemistry

The general synthetic routes used to prepare substituted 1,1,2-tribenzyl-but-1-ene compounds are outlined in Scheme 1. Desoxyanisoin was treated with potassium t-butoxide followed by reflux with ethyl iodide to give **1** in 74% yield. Intermediate **1** was refluxed with the formed Grignard reagent of 4-bromoanisole, then treated with phosphoric acid to yield **2**. Removal of the methoxide groups was accomplished with boron tribromide to give **3**. Isomers **6–7** were synthesized from **1** by treatment with the formed Grignard reagent of bromobenzene followed reflux in phosphoric acid to yield isomers **4–5**. Removal of the two methoxides was accomplished with boron tribromide resulting in isomers **6–7**. Compounds **11–12** were obtained by reaction of desoxyanisoin with glacial acetic acid and hydroiodic acid to give **8** in

90% yield. Dihydroxy **8** was protected using 3,4-dihydro-2H-pyran and p-toluene sulfonic acid to form **9**. Compound **9** was treated with potassium t-butoxide followed by reflux with ethyl iodide to yield **10** in 87%. Compound **10** was refluxed with the formed Grignard reagent of 4-bromophenetole, followed by acid hydrolysis using phosphoric acid to yield isomers **11–12**. Synthesis of **15** proceeded from reaction of anisole with 2-phenylbutyryl chloride to form monomethoxide **13** in 94% yield. Compound **13** was coupled with 4-methoxyphenyl magnesium bromide, by phosphoric acid to produce **14**. The methoxides of **14** were treated with boron tribromide to give dihydroxy **15**.

Pharmacology

We compared and contrasted the estrogen-like properties of the hydroxylated TPEs to promote proliferation in the ERα-positivehuman breast cancer cell line MCF-7:WS8. Compounds were compared with the tamoxifen metabolites 4-OHTAM and endoxifen, which have a high affinity for the ER (because of the appropriately positioned phenolic hydroxyl) but are antiestrogenic because of the alkylaminoethoxy-side chain. To compare the biological activities of the tested TPEs we employed DNA proliferation assays which are described in the materials and methods.

Figure 2 shows that our MCF-7:WS8 human breast cancer cells were exquisitely sensitive to E2 which produced a concentration-dependent increase in growth with maximal stimulation at 1×10^{-11} M. All of the TPE's were potent agonists with the ability to stimulate MCF-7:WS8 breast cancer cell growth, however, their agonist potency was less compared to E2, which had an effective concentration 50% (EC_{50}) of 1×10^{-12} M. The most potent of the phenolic TPEs was bisphenol (**15**) with an EC_{50} of approximately 5×10^{-11} M. The second potent were the E and Z-isomers of the diphenolic TPEs, compounds **6** and **7**, which both had an EC_{50} of approximately 1×10^{-10} M. The triphenolic TPE (**3**) was slightly less active with an EC_{50} of approximately 1.5×10^{-10} M whereas the ethoxy TPE (**12**) was the least potent with an EC_{50} of approximately 4×10^{-9} M. The EC_{50} values for all the tested compounds are outlined in Table 1. The compound **12** was prepared to replicate a molecule without the alkyl nitrogen group of 4-OHTAM or endoxifen and this derivative had reduced estrogenic potency comparison to the other TPEs, however, the molecule remained a full estrogen agonist in our proliferation assays. The metabolites, 4-OHTAM and endoxifen, had no significant agonist effect in MCF-7:WS8 cells, however, these compounds at 1 μM were able to completely inhibit estradiol-stimulated MCF-7:WS8 breast cancer cell growth (Figure 3), thus confirming their role as antagonists/antiestrogens. Similar experiments performed with compounds **3** and **12** showed an inability to block estradiol-stimulated growth in MCF-7:WS8 cells at concentrations up to 1 μM (Figure 3). Based on these findings, compounds **3** and **12** were classified as estrogens with a pharmacology, in this assay, indistinguishable from the natural planar estrogen E2.

It is interesting to note that compounds **6** and **7**, which are the E and Z-isomers of the diphenolic TPEs, were equivalent in their agonistic potency, thus suggesting that isomerization occurs *in vitro* given an equilibrium mixture. This phenomenon has been noted previously with the E isomer of 4-OHTAM [20] but the true pharmacology of the separate isomers was eventually resolved by the synthesis of fixed ring analogs [20, 21]. Both the E and Z isomers of 4-OHTAM are antiestrogenic because they block the proliferation of estradiol-stimulated growth in MCF-7 breast cancer cells and they inhibit estradiol-stimulated prolactin gene activation. The E isomer is however approximately 1/100 the potency of the Z isomer.

To determine the ability of the test TPEs to activate the ER, MCF-7:WS8 cells were transiently transfected with an estrogen response element (ERE)-luciferase reporter gene encoding the firefly reporter gene with 5 consecutive EREs under the control of a TATA promoter. The binding of ligand-activated ER complex at the EREs in the promoter of the luciferase gene activates transcription. The measurement of the luciferase expression levels permits a determination of agonist activity of the TPE:ER complex. Figure 4 shows that all the phenolic

TPEs were estrogenic, but E2 was 100 times more potent than the most potent TPE bisphenol (**15**). The order of potency was as follows: E2 > **15** > **3** > **7** > **6** > **12** > 4-OHTAM. None of the tested TPEs were antiestrogenic in this assay.

Our goal was to confirm and advance the hypothesis that the shape of the estrogen ER complex was different for planar and nonplanar (TPE –like) estrogens. This hypothesis has been advanced independently by ourselves [18, 22] and Gust's group [19]. Through a series of studies using mutant ER expression in an ER negative breast cancer cell line, we found that the mutant D351G ER completely suppressed estrogen-like properties of 4-OHTAM at an endogenous TGFα target gene[17]. Use of this assay led us to classify planar estrogens (DES or E2) as Class I and non planar estrogens (TPE-type) as Class II. A broad group of compound structures were used in this study to establish whether a Class II compound could become non-estrogenic with the D351G ER mutant.

Our series of phenolic TPEs were evaluated in the ER-negative breast cancer cell line T47D:C42 [23] which was transiently transfected with an ERE luciferase plasmid and either the wild-type ER or the D351G mutant ER. Figure 5A shows that in the presence of the wild-type ER all of the tested TPE compounds were potent agonists with the ability to significantly enhance ERE luciferase activity. In contrast, when the D351G mutant ER gene was transfected with the ERE luciferase reporter only the planar E2 was estrogenic whereas the TPEs did not activate the ERE reporter gene (Figure 5B). Overall, these results confirm the importance of Asp351 in ER activation by TPE ligands to trigger estrogen action.

Analysis of the induced fit models for tested TPEs

Data analysis was performed on top ranked poses for each of the tested TPEs and for comparison reasons on 4OHTAM (Figure 6A). The top ranked structure from induced fit for 4OHTAM has a ligand root mean square deviation (RMSD) of 0.55 Å compared with the experimental structure. In addition to the low ligand RMSD there is a good similarity between the 3ert crystal structure and the top ranked structures from docking (Figure 6B), the conformations of D351, E353, R394, T347, H524 and the rest of amino acids which line the binding site are nearly superimposable in both structures. Also, the well known network of H-bonds is formed between 4OHTAM and E353, R394 and water molecules. The most significant difference is that in the top docked pose of 4OHTAM the antiestrogenic chain is moved closer to D351 to form the interaction between the amino group of 4OHTAM and carboxylate of D351. Induced fit docking of the TPE derivatives: **3**, **6**, **7**, **12**, **15** and endoxifen in the ligand binding domain of ERα (3ert) has yielded ligand poses which display a binding mode (Figure 6B) very similar with that of 4OHTAM in the ER binding site (Figure 6A). Thus, the superimposition of the top ranked poses of each ligand onto the 4OHTAM co-crystallized with ERα (binding cavity filled with water) shows the ligands binding to the receptor in a similar mode with 4OHTAM, having the propensity to form the same hydrophobic contacts with the amino acids lining the binding cavity. Furthermore, the complex H-bond network is formed with E353, R394, H524 and a highly ordered water molecule positioned between E353 and R394 (Figure 6B). Interestingly, a H-bond has been noticed between the hydroxyl group of **15**, **3**, **7** and the side chain of T347 is stabilized by an additional interaction with a water molecule from close proximity and precludes the interaction of the ligands with D351. The situation is different when water is removed from the binding site. In this case the OH is shifted so that the H interacts with the carboxylate group of D351 and the HO group of T347 is shifted to form a H-bond with the oxygen. (data not shown). The molecular docking results have shown that most of the compounds form the H-bond network encountered in the case of agonists (E353, R394, H524, water) and display hydrophobic interactions with the amino acids lining the binding site. An interesting interaction is the hydrogen bond with T347 which seems to be stabilized by a water molecule and it was observed in different docking simulations (flexible

and rigid). However, analysis of other ER crystal structures has not revealed additional data to confirm this interaction. Additional work has to be done to verify the hypothesis (docking, binding energy calculations through semiempircal and/or *ab-initio* methods, etc). The interaction with D351 is weak (3.8 – 4 Å) and it was mostly noticed when the simulations were run with the receptor without water in the binding site. This would mean that D351 is exposed and not shielded so it could communicate intrinsic estrogenic properties of the complex to AF-1.

The best poses of the tested TPEs **3**, **6**, **7**, **12**, **15** and endoxifen, obtained from docking simulations ran against the antagonist conformation of the ER, were superimposed on the experimental agonist conformation of the ER (ER co-crystallized with estradiol, PDB code 1GWR) (Figure 7A). This has shown that these ligands are unlikely to be accommodated in the agonist conformation of the ER due to the sterical clashes between "Leu crown", mostly Leu525 and Leu540, helix 12 and ligands as depicted in Figure 7B, indicating, that these ligands most likely bind to ER's conformation more closely related with the antagonist form.

Discussion

The aim of this structure function relationship study was to evaluate the pharmacological properties of synthetic TPEs as estrogens in MCF-7 human breast cancer cells using the DNA proliferation assay and ERE luciferase assays. Our results show that all of the synthesized TPEs possess potent estrogen-like properties in our MCF-7 human breast cancer cells. These TPEs markedly increased cell growth and enhanced ERE luciferase activity. In contrast, the tamoxifen metabolites 4OHTAM and endoxifen, which possess an alkylaminoethoxy sidechain in their structure, failed to induce growth or increase ERE luciferase activity thus confirming their role as antiestrogens.

X-ray crystallography of ER-4OHTAM and ER-Raloxifene complexes demonstrate that the presence of the alkyaminoethoxy sidechain of 4OHTAM is crucial for the ER to gain an antagonistic conformation by displacing the H12 of the receptor by 4OHTAM's bulky sidechain, thus preventing the binding of the coactivators [13]. Based on the results of our proliferation assays and the luciferase assays, it is clear that repositioning of the hydroxyl groups changed the biological potencies of the tested TPE compounds which lowered their estrogenic potency compared to that of E2. However, the fact that these TPEs were able to significantly induce growth and ERE activation in MCF-7:WS8 cells demonstrated that they are still full agonists. The absence of the alkyaminoethoxy sidechain on the tested TPEs does not allow these compounds to act as antiestrogens, like 4-OHTAM or endoxifen, which possesses the alkyaminoethoxy sidechain [13]. However, despite the changes in biological potencies of the tested TPEs, due to repositioning of the hydroxyl groups and addition of the ethoxy group, these compounds also maintained their ability to activate the ERE as was demonstrated in our ERE luciferase assays.

Another interesting aspect in our study is the importance of Asp351 in activation of the ER thereby acting as a molecular test for the presumed structure of the TPE:ER complex. Based on the X-ray crystallography of the ER in complex with 4OHTAM [13] and raloxifene[12], it was determined that the basic side chains of these antiestrogens are in proximity of Asp351 in the ER. It was hypothesized that this interaction with raloxifene actually neutralizes and shields Asp351 preventing it from interacting with ligand-independent activating function 1 (AF-1). In contrast, 4OHTAM possesses some estrogenic activity, because the side chain is too short [13]. Substitution of Asp351 with glycine leads to loss of estrogenic activity of the ER bound with 4OHTAM [17, 24]. Results from ERE luciferase assays in T47:C4:2 cells transiently transfected with wild type and D351G mutant ER expression plasmids demonstrated that wild type ER was activated by all of the tested TPEs, however substitution of Asp351 by Gly

prevented the increase of ERE luciferase activity by all TPEs and only planar E2, which does not interact with Asp351 at all, or exposes it on the surface of the complex, was able to activate ERE in D351G ER transfected cells. This confirms and expands the classification of estrogens, where planar estrogens such as E2 are classified as class I and all TPE-related estrogens are classified as class II estrogens based on the mechanism of activation of the ER [18].

It is important to note that all of the tested TPEs were agonists in our wild type ER assay systems, however, extensive studies of the structure function relationship of phenolic TPEs by Gust and co-workers [25, 26], demonstrated that some of these compounds were potent antagonists in their MCF-7:2A cells stably transfected with an ERE luciferase plasmid. Specifically, these investigators found that compounds 1,1,2-Tris(4-hydroxyphenyl)but-1-ene and 1,1-Bis(4,4′-hydroxyphenyl)-2-phenylbut-1-ene, which correspond to compounds **3** and **15** in this study, were able to completely inhibit estradiol-stimulated ERE luciferase activity at 100 nM. The antagonistic potency of these compounds, however, did not correlate with results from the cytotoxicity assays performed in their wild-type MCF-7 cells [25, 26]. Both compounds 1,1,2-Tris(4-hydroxyphenyl)but-1-ene (designated as **3** in this study) and 1,1-Bis (4,4′-hydroxyphenyl)-2-phenylbut-1-ene (designated as **15** in this study) produced weak cytotoxic effects only at concentrations above 5 uM which were well beyond the concentration range used in our study. Thus it is possible that the variation in findings between our laboratory and that of Gust and coworkers [25, 26] might be due to differences in our in vitro model systems and our experimental design.

Conclusions

We have confirmed and advanced the hypothesis [18, 19, 22] that estrogens can be classified into planar Class I compounds (E2) and non planar Class II compounds (TPEs). Armed with these new tools, we are now poised to examine the biological consequences of estrogen classification based on the shape of the resulting ER complex.

Materials and Methods

Chemistry

1,1,2-Tris(4-hydroxyphenyl)but-1-ene (3)—1,1,2-Tris(4-hydroxyphenyl)but-1-ene (**3**) was synthesized according to the method of Lubczyk, Bachmann and Gust [26].

1,2-Bis(4-methoxyphenyl)butanone (1)

Potassium tert-butoxide (1.35 g, 12 mmol) was added to a solution of desoxyanisoin (2.55 g, 10 mmol) in anhydrous ether under a nitrogen atmosphere and the mixture was stirred for 1 hour. At which time, iodoethane (0.8 ml, 10 mmol) was added dropwise and the mixture was refluxed for 12 hours. Water (40 ml) was added and the product was extracted with ether. The ether extracts were combined, dried over sodium sulfate and evaporated under reduced pressure. The crude product was dissolved in carbon tetrachloride (10 ml) and petroleum ether was added to crystallize unreacted desoxyanisoin. Dexosyanisoin was filtered off and the filtrate was evaporated *in vacuo* to yield **1** as colorless oil (2.11 g; 74%). ^{1}H NMR (CDCl$_3$): δ = 0.88 (t, 3H, J=7.5 Hz); 1.81 (m, 1H); 2.15 (m, 1H); 3.75 (s, 3H, OCH3); 3.82 (s, 3H, CH3); 4.34 (t, 1H, J=7.5 Hz); 6.84 (d, 2H, J=8.7 Hz); 6.88 (d, 2H, J=9.0 Hz); 7.26 (d, 2H, J=9.0 Hz); 7.97 (d, 2H, J=9.0 Hz).

E/Z 4,4′-(1-phenylbut-1-ene-1,2-diyl)bis(methoxybenzene) (4) and (5)

Bromobenzene (1.12 ml, 1.664 g, 10.6 mmol) was added dropwise over 30 minutes to a stirred solution of magnesium turnings (0.26 g, 10.6 mmol) in dry tetrahydrofuran (THF) (10 ml) under a nitrogen atmosphere. Once the Grignard reagent formed and went into solution, **1** (2.03

g, 7.0 mmol) in THF (10 ml) was added dropwise over 60 minutes. The reaction was refluxed for 12 hours, then, quenched with water (10 ml) and the THF removed under reduced pressure. The aqueous layer was extracted with ether (3 × 50 ml). The ether extracts were washed with saturated sodium bicarbonate, water and dried over sodium sulfate. The crude carbinol was refluxed with 85% phosphoric acid (10 ml) in dry THF (20 ml) for 2 hours. The reaction mixture was diluted with water (30 ml) and extracted with of dichloromethane (3 × 50 ml). The dichloromethane layers were washed with sodium bicarbonate, water and dried over sodium sulfate. It was filtered and the solvent removed under reduced pressure yielding a brown oil. Purification by flash chromatography over silica (3.0 × 30 cm) and elution with 200ml of petroleum ether; 300 ml of 5% ether 95% pet ether; 500 ml of 10% ether 90% petroleum ether yielded two isomers. Isomer E **4** (0.322 g; 15% yield) was collected in fractions 17 to 19 while Z isomer **5** was collected in fractions 20 to 28 (0.746 g; 31% yield). ^{1}H NMR E isomer (CDCl$_3$): δ = 0.96 (t, 3H, J=7.5 Hz); 2.49 (q, 2H, J=7.5 Hz); 3.76 (s, 3H); 3.84 (s, 3H); 6.71 (d, 2H, 8.7 Hz); 6.89 (dd, 4H, J=8.7 and 2.1 Hz); 6.88–7.05 (m, 5H,); 7.15 (d, 2H, J=8.7). ^{1}H NMR Z isomer (CDCl$_3$): δ = 0.93 (t, 3H, J=7.5 Hz); 2.44 (q, 2H, J=7.5 Hz); 3.71 (s, 3H); 3.78 (s, 3H); 6.57 (d, 2H, 8.7 Hz); 6.72 (d, 2H, J=8.7 Hz); 6.89 (d, 2H, J=8.7 Hz); 7.05 (d, 2H, J=8.7); 7.22–7.37 (m, 5H).

E/Z 4-(1-(4-hydroxyphenyl)-1-phenylbut-1-en-2-yl)phenol (6) and (7)

Boron tribromide (1.23 ml; 3.25 g; 0.0129 moles) in dichloromethane (5 ml) was added dropwise over 60 minutes to 4,4′-(1-phenylbut-1-ene-1,2-diyl)bis(methoxybenzene) **4** or **5** (0.746, 2.17 mmoles) in dry dichloromethane (20 ml) cooled in a dry ice/ethanol bath while stirring under a nitrogen atmosphere. The solution turned dark immediately and was allowed to warm to room temperature after the addition was complete. The reaction mixture was stirred for a total of 4 days at room temperature. Excess boron tribromide was removed using a nitrogen stream, then, anhydrous methanol (3 × 25 ml) was added and it was evaporated *in vacuo* three times. It was recrystallized from benzene and purified further by preparative HPLC using 70% methanol 30% water. Fractions were collected as follows: E isomer **6** (28 to 39 minutes, 1.814 Abs; 40 mg); Z isomer **7** (41 to 58 minutes, 2.007 Abs; 78 mg). ^{1}H NMR E isomer **6** (MeOD): δ= 0.90 (t, 3H, J=7.5 Hz); 2.47 (q, 2H, J=7.5 Hz); 6.39 (d, 2H, J=8.4 Hz); 6.65 (d, 2H, J=8.7); 6.76 (d, 2H, J=8.4 Hz); 7.02 (d, 2H, J=8.7); 7.07–7.12 (m, 5H). ^{1}H NMR Z isomer **7** (MeOD): δ = 0.90 (t, 3H, J=7.5 Hz); 2.38 (q, 2H, J=7.5 Hz); 6.43 (d, 2H, 8.4 Hz); 6.59 (d, 2H, J=8.4 Hz); 6.66 (d, 2H, J=8.4 Hz); 6.93 (d, 2H, J=8.4 Hz); 7.16–7.32 (m, 5H). MS m/z calculated for C$_{22}$H$_{20}$O$_2$ 315.14 (M-H)$^-$; found 315 for both samples.

1,2-Bis(4-hydroxyphenyl)ethanone (8)

Desoxyanisoin (1.0g; 3.90 mmoles) was dissolved in glacial acetic acid (1 ml) with stirring. Next, hydroiodic acid (5 ml, 36.5 mmoles) was added and the solution was heated to 130–140° C for 4 hours. The reaction mixture was poured into water (50 ml) and the blue-grey colored solid was filtered, washed with water. It was dried *in vacuo* to yield **9** (0.80 g; 90%). Melting point 205–208° C. ^{1}H NMR (MeOD): δ = 4.13 (s, 2H); 6.71 (d, 2H, J=8.7 Hz); 6.83 (d, 2H, J=8.7 Hz); 7.06 (d, 2H, J=8.7 Hz); 7.93 (d, 2H, J=8.7 Hz).

1,2-Bis(4-(tetrahydro-2*H*-pyran-2-yloxy)phenyl)ethanone (9)

1,2-Bis(4-hydroxyphenyl)ethanone (**8**) (700 mg, 3.07 mmoles) was suspended in benzene (35 ml) with stirring under nitrogen atmosphere. Then, 3,4-dihydro-2H-pyran (6 ml, 65.6 mmoles) was added, followed by p-toluenesulfonic acid monohydrate (53 mg, 0.28 mmoles) and the solution was stirred at 0 °C for 4.5 hours. The solution changed from purple to pink to clear. It was poured into saturated sodium bicarbonate solution and extracted with ethyl acetate. The combined ethyl acetate layers were washed with water, dried over magnesium sulfate, and evaporated *in vacuo* to a yellow solid. The residue was triturated with carbon tetrachloride to

remove unreacted pyran. The white solid (548 mg) was collected by filtration and the filtrate was purified by column chromatography over silica (2.7 × 4 on 2.7 × 22). The product was eluted with 100 ml pet ether; 200 ml 10% ether 90% pet ether; 200 ml 20% ether 80% pet ether; 200 ml 30% ether 70% pet ether and 200 ml of 40% ether 60% pet ether. Fractions 33–40 were combined and evaporated *in vacuo* to give 243 mg of additional product (791 mg, 65% yield). ^{1}H NMR (CDCl$_3$): δ = 1.59–2.00 (m, 12H); 3.60 (m, 2H); 3.86 (m, 2H); 4.16 (s, 2H); 5.38 (t, 1H, J=3.0 Hz); 5.50 (t, 1H, J=3.0 Hz); 7.00 (d, 2H, J=8.7 Hz); 7.07 (d, 2H, J=8.7 Hz); 7.17 (d, 2H, J=8.7 Hz); 7.97 (d, 2H, J=9.0 Hz).

1,2-Bis(4-(tetrahydro-2*H*-pyran-2-yloxy)phenyl)butan-1-one (10)

Potassium tert-butoxide 9 (229 mg, 2.04 mmoles) was added to 1,2-bis(4-(tetrahydro-2*H*-pyran-2-yloxy)phenyl)ethanone (**9**) (672 mg, 1.69 mmoles) dissolved in anhydrous THF (25 ml) under a nitrogen atmosphere with stirring. The mixture was stirred at room temperature for 1 hour. Next, iodoethane (0.136 ml 1.70 mmoles) was added dropwise and the reaction mixture was refluxed for 6 hours. After cooling, the THF was removed under reduced pressure. Water (30 ml) was added and the product was extracted with ether. The ether extracts were combined, dried over sodium sulfate and evaporated under reduced pressure to **10** (623 mg, 87% yield). ^{1}H NMR (CDCl$_3$): δ = 0.88 (t, 3H, J=7.2 Hz); 1.60–1.97 (m, 12H); 2.13 (m, 2H, J=7.2 Hz); 3.58 (m, 2H); 3.864 (m, 2H); 4.34 (t, 1H, J=7.2 Hz); 5.34 (t, 1H, J=3.0 Hz); 5.46 (t, 1H, J=3.0 Hz); 6.95 (d, 2H, J=8.4 Hz); 7.01 (d, 2H, J=8.4 Hz); 7.20 (d, 2H, J=8.7 Hz); 7.93 (d, 2H, J=8.7 Hz).

*E/Z(*4-(1-(4-ethoxyphenyl)-1-(4-hydroxyphenyl)but-1-en-2-yl)phenol (11) and (12)

4-Bromophenetole (0.160 ml, 1.11 mmoles) in dry THF (10 ml) was added dropwise over 30 minutes to magnesium turnings (27 mg, 1.11 mmol) with stirring under a nitrogen atmosphere. An iodine crystal was added to initiate the reaction and it was refluxed until the magnesium turnings dissolved. Next, 1,2-bis(4-(tetrahydro-2*H*-pyran-2-yloxy)phenyl)butan-1-one (**10**) (0.311 g; 0.735 mmol) was added and the reaction was refluxed for 12 hours. After cooling, the reaction mixture was evaporated *in vacuo* to an orange residue. Water (20 ml), dichloromethane (20 ml) and acetic acid (1 drop) were added to the orange residue and the aqueous layer was extracted with dichloromethane (3 × 25 ml). The organic extracts were washed with saturated sodium bicarbonate, water and dried over sodium sulfate. Filtration and evaporation provide the crude carbinol, which, was hydrolyzed by refluxing for 2 hours with 85% phosphoric acid (1 ml) in dry THF (10 ml). The reaction mixture was diluted with water (30 ml) and extracted with dichloromethane (3 × 50 ml). The dichloromethane was washed with sodium bicarbonate, water and dried over sodium sulfate. It was filtered and the solvent was removed under reduced pressure to a yellow oil. It was purified by prep HPLC over C-18 Delta Pak column eluting with 40% H$_2$O and 60% MeOH. Flow rate was 100 ml/minute. The elution was monitored by UV set to 254. Two fractions were collected: E isomer **11** (54–64 m, 14 mg) and Z isomer **12** (92–100 m, 16 mg). ^{1}H NMR **11** (CDCl$_3$): δ = 0.92 (t, 3H, J=7.5 Hz); 1.34 (t, 3H, J=6.9 Hz); 2.44 (q, 2H, J=7.5 Hz); 3.90 (q, 2H, J=6.9 Hz); 6.55 (d, 2H, J=8.7 Hz); 6.63 (d, 2H, J=8.4 Hz); 6.76 (d, 2H, J=8.7 Hz); 6.80 (d, 2H, J=8.7 Hz); 6.97 (d, 2H, J=8.7 Hz); 7.12 (d, 2H, J=8.4 Hz). ^{1}H NMR **12** (CDCl$_3$): δ = 0.92 (t, 3H, J=7.5 Hz); 1.40 (t, 3H, J=6.9 Hz); 2.45 (q, 2H, J=7.5 Hz); 4.02 (q, 2H, J=6.9 Hz); 6.49 (d, 2H, J=8.7 Hz); 6.63 (d, 2H, J=8.4 Hz); 6.73 (d, 2H, J=7.8 Hz); 6.86 (d, 2H, J=8.4 Hz); 6.97 (d, 2H, J=8.4 Hz); 7.12 (d, 2H, J=8.7 Hz). MS m/z calculated for $C_{24}H_{24}O_3$ 360; (M-H)$^-$ found 359; (M+H)$^+$ found 361.

1-(4-methoxyphenyl)-2-phenylbutan-1-one (13)—Anisole (5.861 g, 54.2 mmol) and 2-phenylbutyryl chloride (9.90 g, 54.2 mmol) were dissolved in 20 ml of carbon disulfide with stirring under a nitrogen atmosphere. The reaction mixture was cooled in an ice bath while, AlCl$_3$ (7.6 g, 57.0 mmoles) was added keeping the temperature between 10–20 ° C. It was stirred at room temperature for 20 hours. The dark red reaction mixture was poured into ice

and the aqueous layer was extracted with ether (3 × 75 ml). The combined ether layers were washed with 10% KOH, 10% HCl and saturated sodium bicarbonate solutions. The ether layer was then dried over $MgSO_4$ and evaporated under reduced pressure to a yellow solid **18** (13.01 g; 94% yield). Mp 41–42.5 ° C. TLC: ($CHCl_3$) Rf=0.57. NMR ($CDCl_3$): δ= 0.90 (t, 3H, J=7.2 Hz); 1.84 (m, 1H, J=7.2 Hz); 2.19 (m, 1H, J=7.2 Hz); 3.82 (s, 3H); 4.40 (t, 1H, J=7.2 Hz); 6.86 (d, 2H, J=9 Hz); 7.16–7.41 (m, 5H); 7.96 (d, 2H, J=9 Hz).

1,1-Bis(4,4'-methoxyphenyl)-2-phenylbut-1-ene (14)

Compound **18** (1.0g, 3.93 mmoles) in 10 ml of THF was added dropwise over 15 minutes to a 1M THF solution of 4-methoxyphenyl magnesium bromide (5.8 ml, 5.8 mmoles) cooled in an ice bath under a nitrogen atmosphere with stirring. The solution was refluxed for 17.5 hours. The reaction mixture was poured into 20ml water and 8ml 6N acetic acid. The aqueous layer was extracted with ether (3 × 50 ml). The ether extracts were washed with saturated sodium bicarbonate, brine, dried over sodium sulfate and evaporated under reduced pressure to oil. The crude carbinol was refluxed with 85% phosphoric acid (10 ml) in dry THF (20 ml) for 2 hours. The reaction mixture was diluted with water (60 ml) and extracted with of dichloromethane (3 × 50 ml). The dichloromethane layers were washed with sodium bicarbonate, water and dried over sodium sulfate. The solvent removed under reduced pressure yielding a cream solid. Purification by flash chromatography over silica (2.7 × 37 cm) and elution with 500 ml hexanes gave pure **19** in fractions 7–18, which were combined and evaporated *in vacuo*. Yield 1.30 g (96%). Mp 116–118 ° C. TLC: ($CHCl_3$) Rf=0.68. NMR ($CDCl_3$):δ = 0.93 (t, 3H, J=7.5 Hz); 2.48 (q, 2H, J=7.5 Hz); 3.68 (s, 3H); 3.83 (s, 3H); 6.54 (d, 2H, J=9 Hz); 6.77 (d, 2H, J=9 Hz); 6.88 (d, 2H, J=9 Hz); 7.07–7.19 (m, 7H).

1,1-Bis(4,4'-hydroxyphenyl)-2-phenylbut-1-ene (15)

Compound **19** (1.9 g, 3.79 mmoles) in 18ml dry dichloromethane was cooled to −55 ° C under a nitrogen atmosphere with stirring. Then, BBr_3 (2.17ml, 22.95 mmoles) in 10ml dichloromethane was added over 30 minutes while the temperature was kept at −55 ° C. The reaction mixture was stirred at room temperature for 90 hours. The reaction was quenched by addition of methanol. The methanol was evaporated and this was performed three more times which resulted in a green residue. The crude product was purified by flash chromatography on a silica column (4×26 cm) equilibrated with hexane. It was eluted with chloroform:methanol (85:15) and 20ml fractions were collected. Fractions 18–27 were combined and evaporated under reduced pressure. The resulting solid was recrystallized from chloroform but contained a small impurity by HPLC. It was purified by prep HPLC over C-18 Delta Pak column eluting with 20% H_2O and 80% MeOH. Flow rate was 30 ml/minute. The UV detector was set to 254λ. The product was collect from 20–24 minutes and the solvent was evaporated *in vacuo* to give **20** (75 mg, 5% yield). Mp 206–206.5 ° C. TLC: ($CHCl_3$ 9:methanol 1) Rf=0.50. NMR ($CDCl_3$): δ= 0.92 (t, 3H, J=7.5 Hz); 2.47 (q, 2H, J=7.5 Hz); 4.48 (s, 1H); 4.71 (s. 1H); 6.46 (d, 2H, J=8.4 Hz); 6.73 (d, 2H, J=8.4 Hz); 6.81 (d, 2H, J=8.4 Hz); 7.10–7.16 (m, 7H).

Cell culture—The ER-positive human breast cancer cell line MCF-7:WS8 and the ER-negative breast cancer cell line T47D:C4:2 were used in our study. MCF-7:WS8 cells were cloned from wild type MCF-7 cells that were originally obtained from Dr. Dean Edwards (University of Texas, San Antonio, TX) and were maintained in phenol-red RPMI 1640 medium containing 10% fetal bovine serum (FBS), 2mM glutamine, penicillin at 100 units/mL, streptomycin at 100 μg/mL, 1 X non-essential amino acids (all from Invitrogen, Carlsbad, CA), and bovine insulin at 6 ng/mL (Sigma-Aldrich, St. Louis, MO). The hormone-independent T47D:C4:2 cells were subcloned from T47D:C4 clones of T47D cells that were originally obtained from the ATCC (Rockville, MD, USA). The T47D:C4:2 cells are ER-negative hormone-independent cells and they do not re-express ERα following growth in estrogen-containing media[23]. T47D:C4:2 cells were maintained in estrogen-free RPMI 1640

medium, containing 10% dextran charcoal-stripped fetal bovine serum (SFS). All cells were cultured in T185 culture flasks (Nalge Nunc International, Rochester, NY, USA) and passaged twice a week in 1:4 ratio. All cultures were grown in 5%CO2, 37°C.

Cell proliferation assays—MCF-7:WS8 cells were cultured in estrogen-free medium (phenol red-free RPMI 1640 media supplemented with 10% charcoal-stripped FBS) for 4 days before beginning the proliferation assay. On day 0 of the experiment, MCF-7:WS8 cells were seeded in estrogen-free RPMI media containing 10% SFS at a density of 20,000 cells per well respectively in Nunclon™Δ Surface 24-well plates (Nalge Nunc International, Rochester, NY, USA). After 24h cells were treated with various concentrations of the tested compounds, prepared via serial dilutions. All concentration points were performed in triplicate. The compound-containing medium was changed on days 3 and 5, and the experiment was stopped on day 7. Cells were washed with cold PBS (Invitrogen, Carlsbad, CA, USA) at least twice and analyzed with Fluorescent DNA quantification kit (Bio-Rad, Hercules, CA, USA) according to manufacturers instructions, and samples were read on Mithras LB540 fluorometer/luminometer (Berthold Technologies, Oak Ridge, TN, USA) in black wall 96-well plates (Nalge Nunc International, Rochester, NY, USA).

DNA plasmids—Estrogen Response Element activity was determined via Luciferase assays with pERE(5X)TA-ffLuc and pTA-srLuc reporter plasmids. These plasmids contained the TATA-box basal promoter firefly and the *Renilla* luciferase reporter genes, respectively, and were constructed by insertion via HindIII linkers of the nucleotides −31 and +31 region of the herpes simplex virus thymidine kinase promoter into pGL3-Basic and phRG-B (Promega, Madison, WI, USA) [27]. For transient expression of wild-type ERα and 351 aspartate-to-glycine-substituted mutant ERα, pSG5HEGO and pSG5D351GER plasmids were used respectively. pSG5HEGO was originally provided by Professor Pierre Chambon, University of Strasbourg, France, and pSG5D351GER was generated using QuichChange Site-Directed Mutagenesis Kit (Stratagene, La Jolla, CA, USA) and pSG5HEGO as a template [17]. All plasmids for this study were purified using HiSpeed Plasmid Maxi Kit (Qiagen, Valencia, CA, USA), and were grown via OneShot TOP10 Chemically Competent *E. coli* cells (Invitrogen, Carlsbad, CA, USA).

Transient transfections and luciferase activity assays—MCF-7:WS8 cells were cultured in estrogen-free RPMI media for 24 h prior to transfection. On the day of the experiment cells were seeded in estrogen-free media at a density of 100,000 cells per well in 24-well plates. After 24 h, MCF-7:WS8 cells were transfected with 28.8 μg of pERE(5X)TA-ffLuc and 9.6 μg of pTA-srLuc reporter plasmids, using 3 μl of TransIT-LT1 transfection reagent (Mirus Biolabs, Madison, WI, USA) per 1 μg of plasmid DNA in 52.5 mL of OPTI-MEM serum-free media (Invitrogen, Carlsbad, CA, USA). Transfection mix containing transfection complexes of the transfection reagent and plasmid DNA in OPTI-MEM media was added to cell in growth media to a final concentration of 0.3 μg pERE(5X)TA-ffLuc and 0.1 μg of pTA-srLuc reporter plasmids per well. After 18 hours, transfection reagents were removed and fresh media was added. Cells were then treated with the various test compounds for 24 hours. At the indicated time point, cells were washed once with cold PBS (Invitrogen, Carlsbad, CA, USA), lysed, and ERE luciferase activity was determined using the Dual-Luciferase Reporter Assay System (Promega, Madison, WI, USA) according to manufacturers recommendations. Samples were then read on a Mithras MB540 fluorometer/luminometer (Berthold Technologies, Oak Ridge, TN, USA).

T47D:C4:2 cells were seeded in estrogen-free RPMI 1640 media at a density of 200,000 cells per well in 24-well plates. T47D:C4:2 cells are ER-negative cells, therefore these cells were transiently transfected with wild-type ERα (pSG5HEGO) or D351G mutant ERα (pSG5D351GER), along with pERE(5X)TA-ffLuc and pTA-srLuc reporter plasmids.

Transfection mix contained 7.2 μg of pSG5HEGO or 7.2 μg of pSG5D351GER, 7.2 μg of pERE(5X)TA-ffLuc, and 2.4 μg of pTA-srLuc reporter plasmids, and 3 μl of FuGene HD transfection reagent (Roche Diagnostics, Indianapolis, IN, USA) per 1 μg of plasmid DNA, and 13 mLs of OPTI-MEM serum-free media (Invitrogen, Carlsbad, CA, USA) for 1 × 24-well plate. Transfection complexes of the reagent and plasmid DNA were added to cells in growth media to a final concentration of 0.3 μg of pSG5HEGO or 0.3 μg of pSG5D351GER, 0.3 μg of pERE(5X)TA-ffLuc and 0.1 μg of pTA-srLuc per well. After 18 hours, transfection reagents were removed and fresh media was added. Cell were then treated with the various test compounds for 24 hours and ERE luciferase activity was determined as described above.

Reagents and supplies—Estradiol (E2), 4-hydroxy-tamoxifen (4OHTAM), Bovine Insulin, was obtained from Sigma, St. Louis, MO, USA. Endoxifen (Z-isomer) was a kind gift from Dr. James Ingle (Mayo Clinic). Fetal Bovine Serum (FBS), 2mM glutamine, penicillin at 100 units/mL, streptomycin at 100 μg/mL, 1 X non-essential amino acids, RPMI 1640 with phenol-red media, PBS buffer, RPMI 1640 phenol-red-free media, OPTI-MEM serum-free media were all obtained from Invitrogen, Carlsbad, CA, USA. Fluorescent DNA quantification kit obtained from Bio-Rad, Hercules, CA, USA. HiSpeed Plasmid Maxi Kit was obtained from Qiagen, Valencia, CA, USA. TransIT-LT1 transfection reagent was obtained from Mirus Biolabs, Madison, WI, USA. FuGene HD transfection reagent was obtained from Roche Diagnostics, Indianapolis, IN, USA. Dual-Luciferase Reporter Assay System was obtained from Promega, Madison, WI, USA. Anhydrous ether was purchased from Fisher. Potassium tert-butoxide, desoxyanisoin, magnesium turnings, bromobenzene, boron tribromide, anhydrous methylene chloride, 3,4-dihydro-2H-pyran, oxalyl chloride, N,O-dimethylhydroxylamine, aluminum chloride and cyclohexene were purchased from Acros. Ethyl iodide, hydroiodic acid (55% ACS unstablized), p-toluene sulfonic acid monohydrate, 2-fluoro-3-trifluoromethylbenzoic acid, 2,4-dimethoxymagnesium bromide (0.5 M solution in THF), anisole, 2-phenylbutyryl chloride, phenyl magnesium bromide (1 M solution in THF), sodium hydride (60% in mineral oil), and allylbromide was purchased from Aldrich. Carbon disulfide was purchased from Baker. THF was distilled and stored over calcium hydride. Benzene was distilled from calcium hydride and stored over molecular sieves. Flash chromatography was run using Whatman 230–400 mesh silica gel 60. Preparative chromatography was run on a Waters Delta Prep 3000 HPLC system using a prep pak C-18 delta-pak column (47 × 300 mm). UV detection was set at 254λ. Flow rate was 50 ml per minute. ^{1}H NMR was performed on a Bruker WB Advance 300 Mhz instrument. MS analysis performed by HT Laboratories (San Diego, CA) using electrospray ionization. LC-MS was performed using a Waters 2545 binary gradient module and a 2487 dual wavelength detector set to 254 and 365, a 2424 ELS detector and a 3100 MS detector. The gradient was linear 5% MeOH 95% H_2O to 95% MeOH 5% H_2O over 20 minutes. The column was a Waters Delta Pak C-18 15u 100A 3.9 × 300mm (catalog number 11797) run at a flow rate of 0.8 ml per minute. The purity of all compounds was determined by LC-MS to be 95% or greater.

Molecular modeling

The coordinates for the antagonist conformation of human ER ligand binding domain co-crystallized with 4OHTAM were extracted from the RCSB Protein Data Bank (PDB) [28], entry 3ert was selected for further modeling with ER in antagonist conformation and 1GWR was selected for modeling of the ER in the agonist conformation. The protein was prepared for the docking experiments using the Protein Preparation Workflow (Protein Preparation Wizard, Schrödinger, LLC, Portland, OR) implemented in Schrödinger suite and accessible from within the Maestro program (Maestro 8.5, Schrödinger, LLC, Portland, OR). Briefly, the hydrogen atoms were added, water molecules beyond 5 Å from the ligand were deleted and the orientation of hydroxyl groups, Asn, Gln and the protonation state of His were optimized to maximize hydrogen bonding. All Asp, Glu, Arg and Lys residues were left in their charged state. Finally,

the ligand-protein complex was refined with a restrained minimization performed by Impref utility which is based on the Impact molecular mechanics engine (Impact 4.5, Schrödinger, LLC, Portland, OR) and the OPLS_2001 force field, setting a max RMSD of 0.30.

Ligands preparation for docking was performed with LigPrep (LigPrep 2.1, Schrödinger, LLC, Portland, OR) application which consists of a series of steps that perform conversions, apply corrections to the structure, generate ionization states and tautomers, and optimize the geometries.

Molecular docking was performed using Glide 4.5 (Glide 4.5, Schrödinger, LLC, Portland, OR) followed by the Induced Fit protocol (Induced Fit protocol, Schrödinger, LLC, Portland, OR) which is intended to circumvent the inflexible binding site and accounts for the side-chain or backbone movements, or both, upon ligand binding [29]. In the first stage of the IFD protocol, softened-potential docking step, 20 poses per ligand were retained. In the second step, for each docking pose a full cycle of protein refinement was performed, with Prime 1.6 (Prime 1.6, Schrödinger, LLC, Portland, OR), on all residues having at least one atom within 8 Å of an atom in any of the 20 ligand poses. The Prime refinement starts with a conformational search and minimization of the side chains of the selected residues and after convergence to a low-energy solution, an additional minimization of all selected residues (side chain and backbone) is performed with the truncated-Newton algorithm using the OPLS parameter set and a surface Generalized Born implicit solvent model. The obtained complexes are ranked according to Prime calculated energy (molecular mechanics and solvation) and those within 30 kcal/mol of the minimum energy structure are used in the last step of the process, redocking with Glide 4.5 (extended precision) and scoring. In the final round the ligands used in the first docking step is redocked into each of the receptor structures retained from the refinement step. The final ranking of the complexes is done by a composite score which accounts for the receptor-ligand interaction energy (GlideScore) and receptor strain and solvation energies (Prime energy) [29].

Acknowledgments

Abbreviations

ER	estrogen receptor
SERM	selective estrogen receptor modulators
TAM	tamoxifen
4OHTAM	4-hydroxytamoxifen
LBD	ligand binding domain
E2	17β-estradiol
DES	diethylstilbestrol
AF	activating function
TPE	triphenylethylene
EC_{50}	effective concentration 50%
ERE	estrogen response element

RMSD	root mean square deviation
THF	tetrahydrofuran
RPMI	Roswell Park Memorial Institute
FBS	fetal bovine serum
SFS	stripped fetal bovine serum
PBS	phosphate buffered saline
OPTI-MEM	Optimum Eagle's Minimum Essential Media
RCSB	Research Collaboratory for Structural Bioinformatics
PDB	Protein Data Bank
OPLS	optimized potential for liquid simulations
IFD	induced fit

References

1. Cancer Facts and Figures. 2009. www.cancer.org

2. Russo IH, Russo J. Role of hormones in mammary cancer initiation and progression. J Mammary Gland Biol Neoplasia 1998;3:49–61. [PubMed: 10819504]

3. EBCTCG. Tamoxifen for early breast cancer: an overview of the randomised trials. Early Breast Cancer Trialists' Collaborative Group. Lancet 1998;351:1451–1467. [PubMed: 9605801]

4. EBCTCG. Effects of chemotherapy and hormonal therapy for early breast cancer on recurrence and 15-year survival: an overview of the randomised trials. Lancet 2005;365:1687–1717. [PubMed: 15894097]

5. Jordan VC. Tamoxifen: catalyst for the change to targeted therapy. Eur J Cancer 2008;44:30–38. [PubMed: 18068350]

6. Fisher B, Costantino JP, Wickerham DL, Redmond CK, Kavanah M, Cronin WM, Vogel V, Robidoux A, Dimitrov N, Atkins J, Daly M, Wieand S, Tan-Chiu E, Ford L, Wolmark N. Tamoxifen for prevention of breast cancer: report of the National Surgical Adjuvant Breast and Bowel Project P-1 Study. J Natl Cancer Inst 1998;90:1371–1388. [PubMed: 9747868]

7. Harper MJ, Walpole AL. Contrasting endocrine activities of cis and trans isomers in a series of substituted triphenylethylenes. Nature 1966;212:87. [PubMed: 5965580]

8. Harper MJ, Walpole AL. A new derivative of triphenylethylene: effect on implantation and mode of action in rats. J Reprod Fertil 1967;13:101–119. [PubMed: 6066766]

9. Robson JM, Schonberg A. Estrous reactions, including mating, produced by triphenyl ethylene. Nature 1937;140:196.

10. Jordan VC, Collins MM, Rowsby L, Prestwich G. A monohydroxylated metabolite of tamoxifen with potent antioestrogenic activity. J Endocrinol 1977;75:305–316. [PubMed: 591813]

11. Johnson MD, Zuo H, Lee KH, Trebley JP, Rae JM, Weatherman RV, Desta Z, Flockhart DA, Skaar TC. Pharmacological characterization of 4-hydroxy-N-desmethyl tamoxifen, a novel active metabolite of tamoxifen. Breast Cancer Res Treat 2004;85:151–159. [PubMed: 15111773]

12. Brzozowski AM, Pike AC, Dauter Z, Hubbard RE, Bonn T, Engstrom O, Ohman L, Greene GL, Gustafsson JA, Carlquist M. Molecular basis of agonism and antagonism in the oestrogen receptor. Nature 1997;389:753–758. [PubMed: 9338790]

13. Shiau AK, Barstad D, Loria PM, Cheng L, Kushner PJ, Agard DA, Greene GL. The structural basis of estrogen receptor/coactivator recognition and the antagonism of this interaction by tamoxifen. Cell 1998;95:927–937. [PubMed: 9875847]

14. Levenson AS, Tonetti DA, Jordan VC. The oestrogen-like effect of 4-hydroxytamoxifen on induction of transforming growth factor alpha mRNA in MDA-MB-231 breast cancer cells stably expressing the oestrogen receptor. Br J Cancer 1998;77:1812–1819. [PubMed: 9667651]

15. Levenson AS, Catherino WH, Jordan VC. Estrogenic activity is increased for an antiestrogen by a natural mutation of the estrogen receptor. J Steroid Biochem Mol Biol 1997;60:261–268. [PubMed: 9219916]

16. Levenson AS, Jordan VC. The key to the antiestrogenic mechanism of raloxifene is amino acid 351 (aspartate) in the estrogen receptor. Cancer Res 1998;58:1872–1875. [PubMed: 9581827]

17. MacGregor Schafer J, Liu H, Bentrem DJ, Zapf JW, Jordan VC. Allosteric silencing of activating function 1 in the 4-hydroxytamoxifen estrogen receptor complex is induced by substituting glycine for aspartate at amino acid 351. Cancer Res 2000;60:5097–5105. [PubMed: 11016635]

18. Jordan VC, Schafer JM, Levenson AS, Liu H, Pease KM, Simons LA, Zapf JW. Molecular classification of estrogens. Cancer Res 2001;61:6619–6623. [PubMed: 11559523]

19. Gust R, Keilitz R, Schmidt K. Investigations of new lead structures for the design of selective estrogen receptor modulators. J Med Chem 2001;44:1963–1970. [PubMed: 11384241]

20. Jordan VC, Koch R, Langan S, McCague R. Ligand interaction at the estrogen receptor to program antiestrogen action: a study with nonsteroidal compounds in vitro. Endocrinology 1988;122:1449–1454. [PubMed: 3345720]

21. Murphy CS, Langan-Fahey SM, McCague R, Jordan VC. Structure-function relationships of hydroxylated metabolites of tamoxifen that control the proliferation of estrogen-responsive T47D breast cancer cells in vitro. Mol Pharmacol 1990;38:737–743. [PubMed: 2233701]

22. Bentrem D, Fox JE, Pearce ST, Liu H, Pappas S, Kupfer D, Zapf JW, Jordan VC. Distinct molecular conformations of the estrogen receptor alpha complex exploited by environmental estrogens. Cancer Res 2003;63:7490–7496. [PubMed: 14612550]

23. Pink JJ, Bilimoria MM, Assikis J, Jordan VC. Irreversible loss of the oestrogen receptor in T47D breast cancer cells following prolonged oestrogen deprivation. Br J Cancer 1996;74:1227–1236. [PubMed: 8883409]

24. Levenson AS, MacGregor Schafer JI, Bentrem DJ, Pease KM, Jordan VC. Control of the estrogen-like actions of the tamoxifen-estrogen receptor complex by the surface amino acid at position 351. J Steroid Biochem Mol Biol 2001;76:61–70. [PubMed: 11384864]

25. Lubczyk V, Bachmann H, Gust R. Investigations on estrogen receptor binding. The estrogenic, antiestrogenic, and cytotoxic properties of C2-alkyl-substituted 1,1-bis(4-hydroxyphenyl)-2-phenylethenes. J Med Chem 2002;45:5358–5364. [PubMed: 12431063]

26. Lubczyk V, Bachmann H, Gust R. Antiestrogenically active 1,1,2-tris(4-hydroxyphenyl)alkenes without basic side chain: synthesis and biological activity. J Med Chem 2003;46:1484–1491. [PubMed: 12672249]

27. Ariazi EA, Kraus RJ, Farrell ML, Jordan VC, Mertz JE. Estrogen-related receptor alpha1 transcriptional activities are regulated in part via the ErbB2/HER2 signaling pathway. Mol Cancer Res 2007;5:71–85. [PubMed: 17259347]

28. Berman HM, Westbrook J, Feng Z, Gilliland G, Bhat TN, Weissig H, Shindyalov IN, Bourne PE. The Protein Data Bank. Nucleic Acids Res 2000;28:235–242. [PubMed: 10592235]

29. Sherman W, Day T, Jacobson MP, Friesner RA, Farid R. Novel procedure for modeling ligand/receptor induced fit effects. J Med Chem 2006;49:534–553. [PubMed: 16420040]
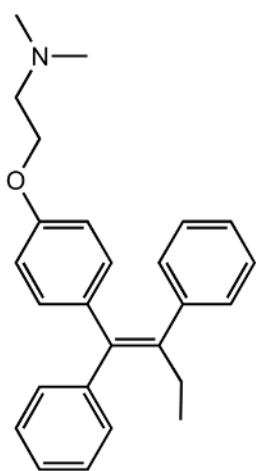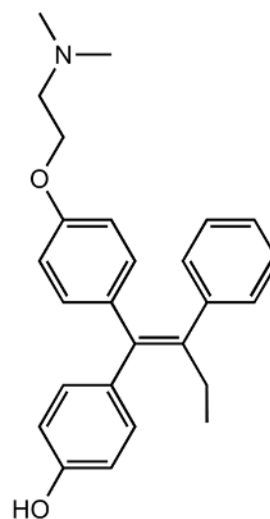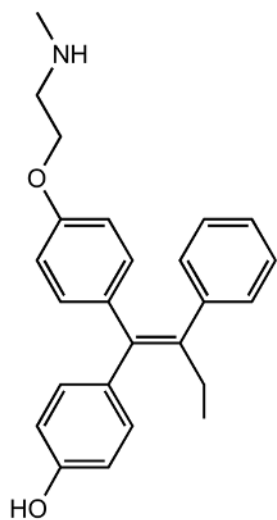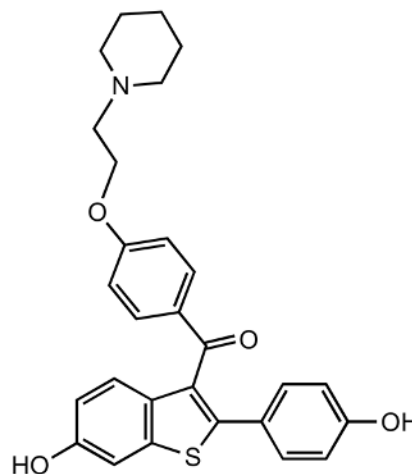
tamoxifen

4-OH tamoxifen

endoxifen

raloxifene

Figure 1.
The formula of tamoxifen and its hydroxylated metabolites endoxifen, and 4OHTAM. The related SERM raloxifene is shown for comparison.
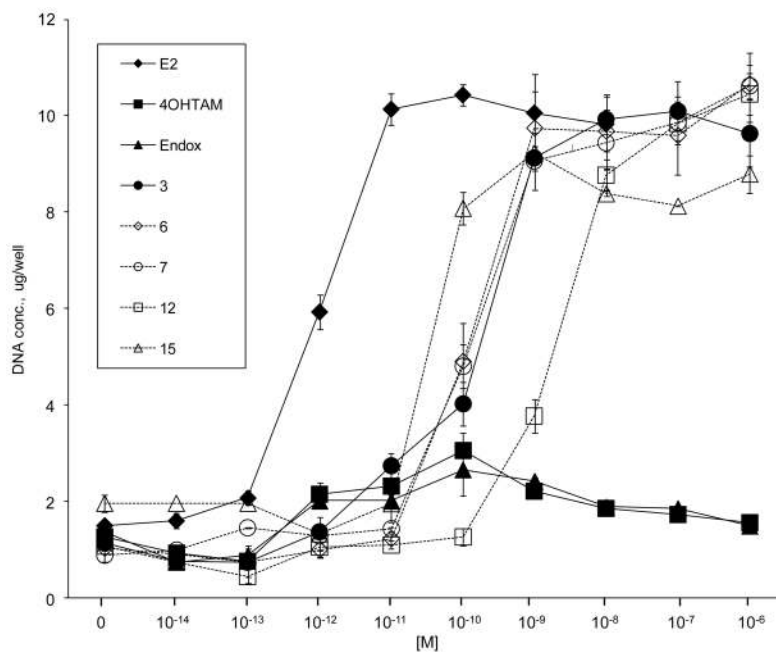
Figure 2.
Effects of E2, test TPEs **3**, **6**, **7**, **12** and **15**, and antiestrogens 4OHTAM and endoxifen on the proliferation of MCF-7:WS8 breast cancer cells. Cells were treated with the indicated compounds for 7 days.
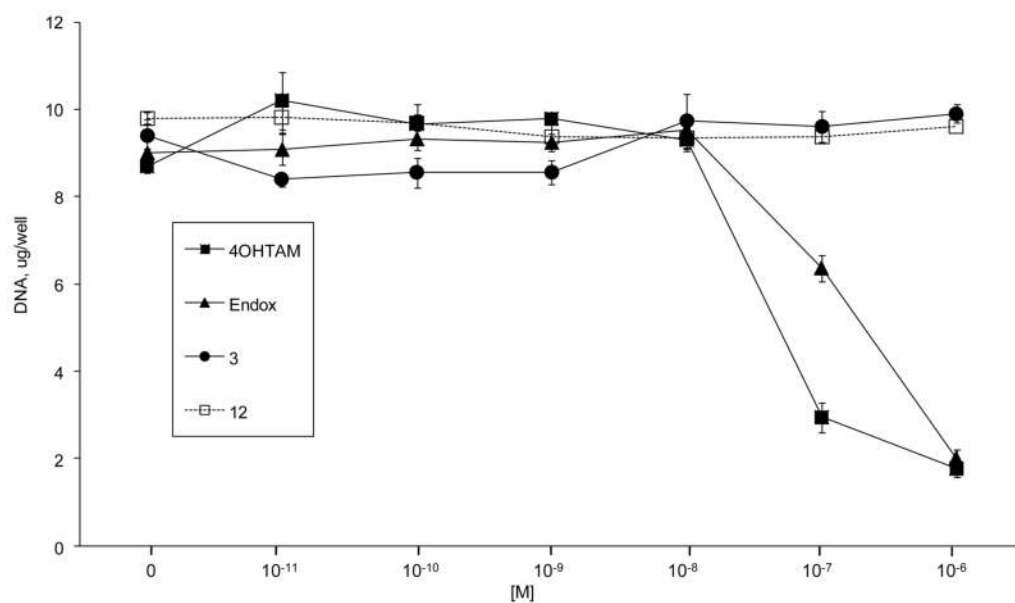
Figure 3.
The ability of the tested TPEs **3** and **12** and 4OHTAM and endoxifen to inhibit estradiol-stimulated MCF-7:WS8 breast cancer cell growth. Cells were treated with indicated compounds for 7 days.
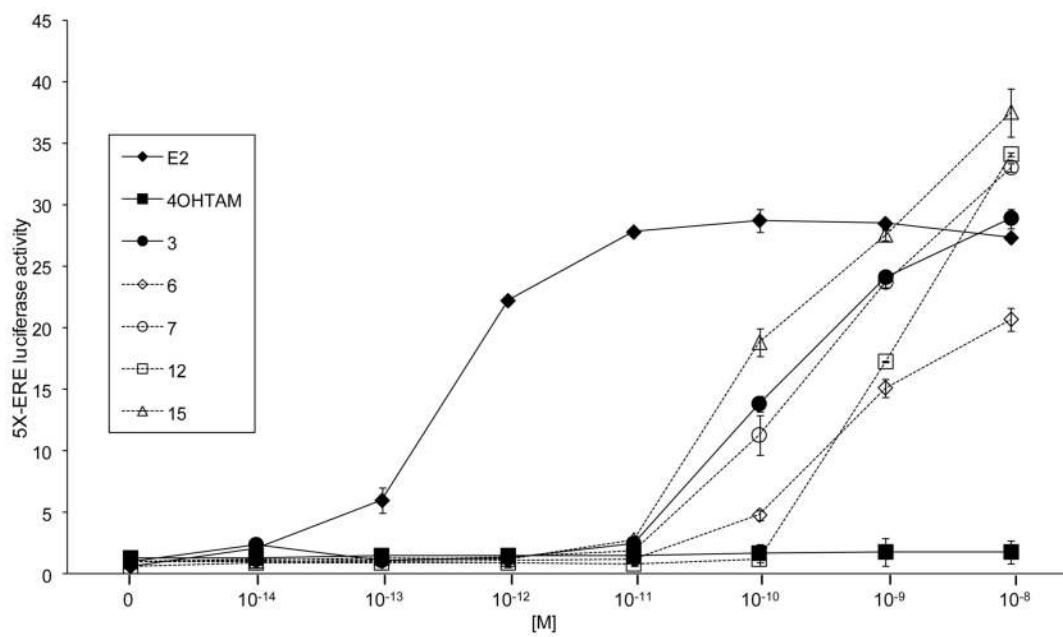
Figure 4.
ERE luciferase assay in MCF-7:WS8 cells transiently transfected with an ERE luciferase construct, and treated with E2, test TPEs **3**, **6**, **7**, **12** and **15**, and 4OHTAM.
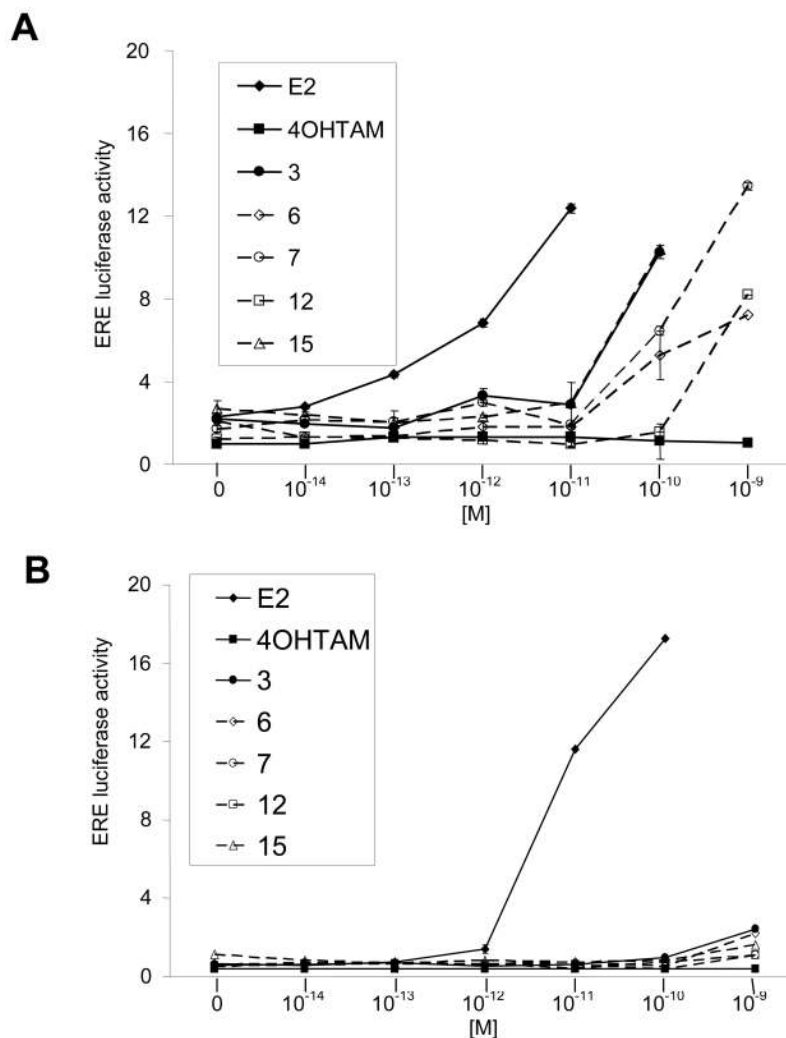
Figure 5.
Luciferase assay in ER-negative T47D:C4:2 cells, transiently transfected with ERE luciferase and wild type (**A**) and D351G (**B**) mutant ER constructs respectively, and treated with E2, tested TPEs **3**, **6**, **7**, **12** and **15**, and 4OHTAM. Results demonstrate that substitution of Asp351 to Gly in ER, abrogates the agonistic activity on all tested TPEs (class II estrogens), except planar E2 (class I estrogen).

Figure 6A.
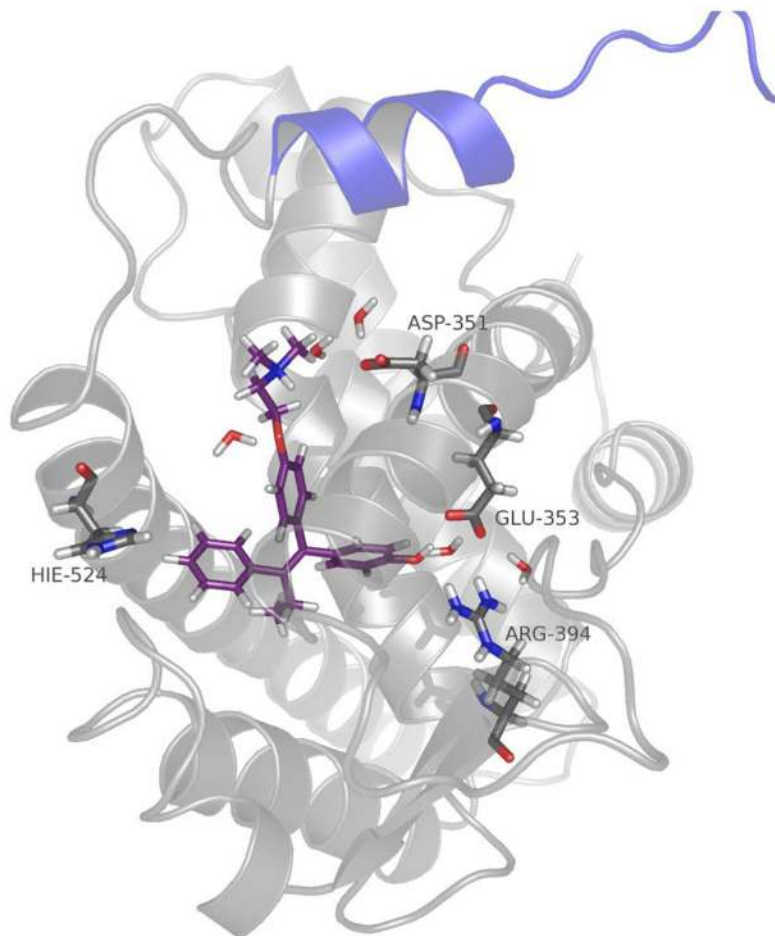
Figure 6B.
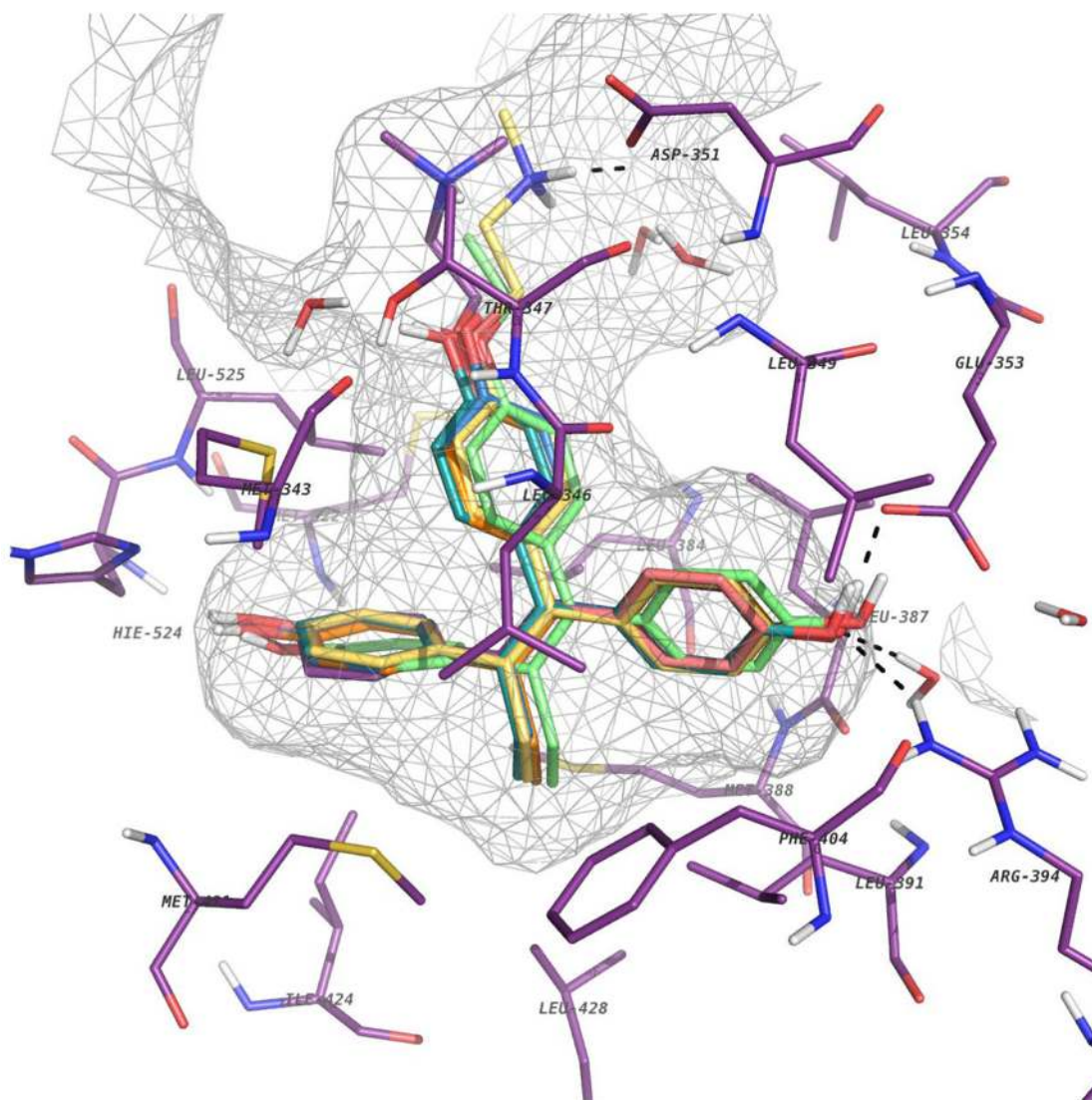
Figure 6.
Figure 6A: Cartoon representation of the human ER alpha ligand binding domain complexed with 4-hydroxy tamoxifen, the antagonist conformation of the receptor. Helix 12 is depicted in blue, the amino acids involved in the H-bond network with the ligand are displayed as sticks and the ligand is colored in purple.
Figure 6B: Molecular docking of TPE derivatives into the binding site of ERalpha. For comparison reason the top ranked ligand-protein complex is superimposed on the crystal structure of the receptor co-crystallized with 4-OHT; the amino acids lining the biding sites of both complexes are shown and the complex H-bond network between ligand and the binding site is displayed. The induced fit docking poses of the ligands are colored as follow: **15** in cyan, **3** in blue, **6** in orange, **7** in pink, **12** in green, Endoxifen in yellow, while the crystal structure is depicted in purple.

Figure 7A.
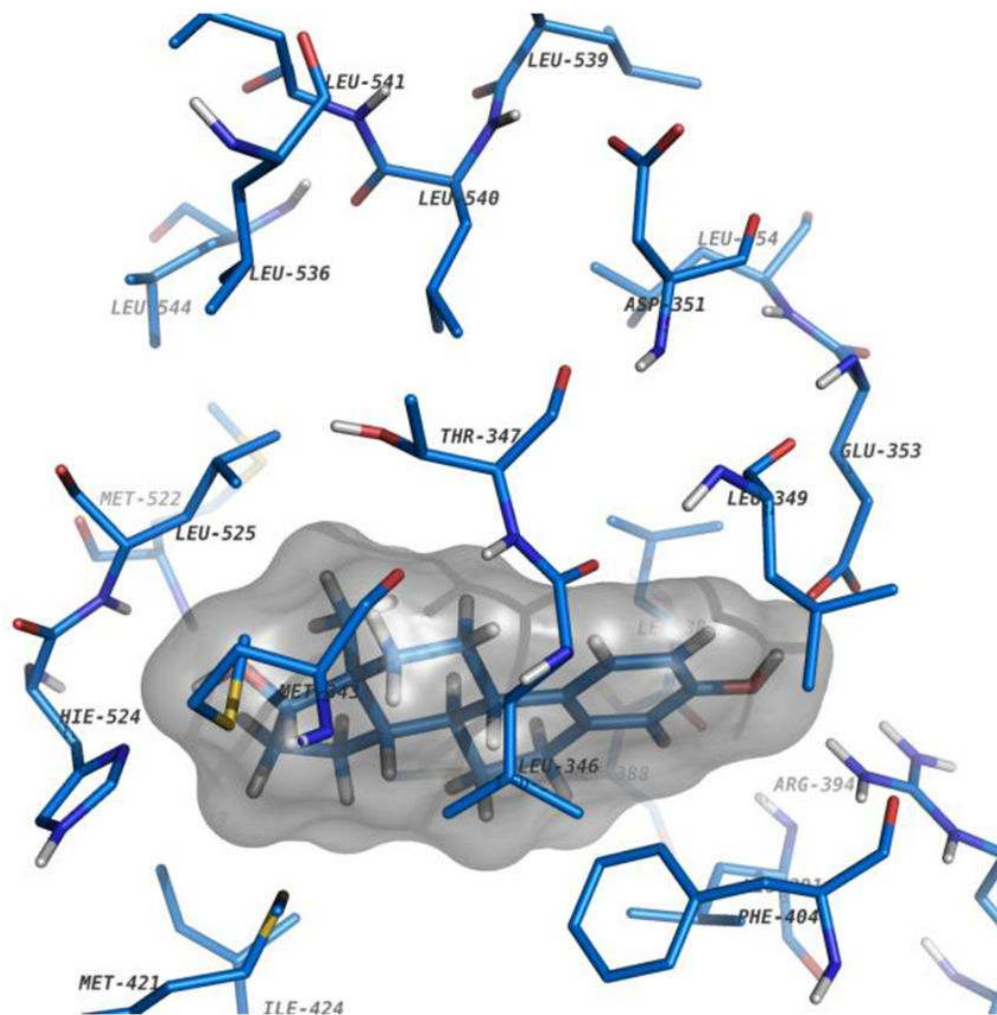
Figure 7B.
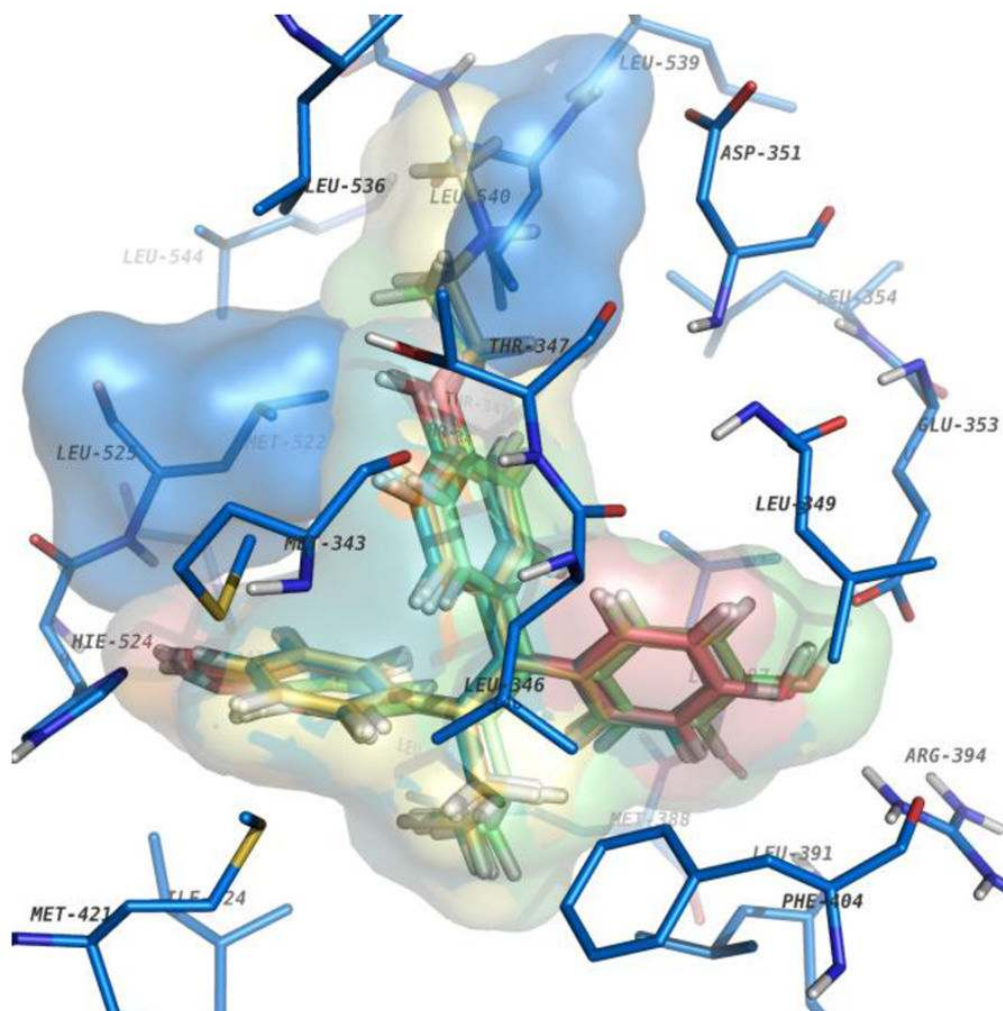
Figure 7.
Figure 7A: View of ERalpha binding cavity. The X-ray crystal structure of ERalpha complexed with estradiol (PDB code 1GWR), the agonist conformation of the receptor. The amino acids lining the binding site are depicted as sticks colored by element. The color code is blue for carbon, red for oxygen, gray for nitrogen and yellow for sulfur. The ligand is represented as sticks having the same colored code like the receptor and the ligand's surface is colored in gray.
Figure 7B: View of ERalpha binding cavity. The best poses of BisPhen, TriOH_TPE, E_DiOH_TPE, Z_DiOH_TPE, Z_4Ethox_DiOH_TPE, Endox obtained from docking simulations ran against the antagonist conformation of the receptor, are superimposed on the agonist conformation of the receptor, ERalpha co-crystallized with estradiol (PDB code 1GWR). The amino acids involved in steric clashes with the ligands, Leu525 and Leu540, are depicted as molecular surfaces colored in blue while the rest of amino acids lining the binding site are depicted as sticks colored by element, the color code is blue for carbon, red for oxygen, gray for nitrogen and yellow for sulfur. The ligands are represented in sticks with the associated molecular surfaces. They respect the same coloring code with the exception of carbons which

are colored as follow: BisPhen in cyan, TriOH_TPE in blue, E_DiOH_TPE in orange, Z_DiOH_TPE in pink, Z_Ethox_DiOH_TPE in green, Endoxifen in yellow. For clarity, waters and hydrogen atoms were omitted from the binding site.
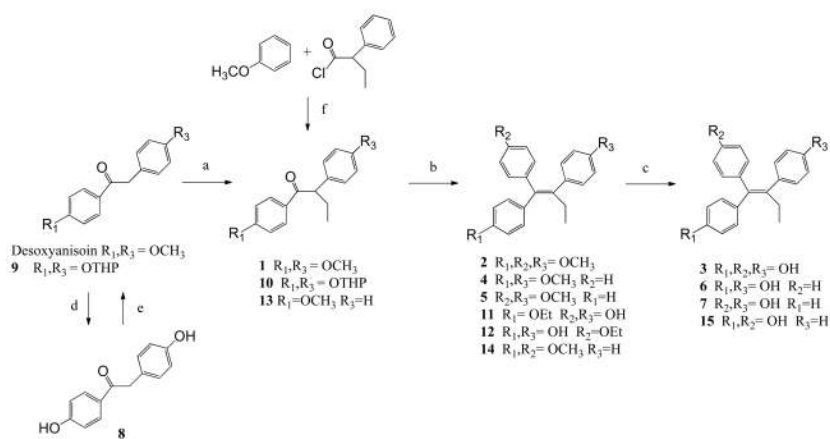
Scheme 1. Synthesis of substituted 1,1,2-tribenzyl-but-1-ene compounds
Reaction conditions: (a) KOtBu, ether, 1 hr, then, EtI, reflux 12 hrs; (b) 4-BrMgC$_6$H$_4$R$_2$, THF, refluxed 12 hrs, then, H$_3$PO$_4$, refluxed 2 hrs; (c) BBr$_3$, CH$_2$Cl$_2$, 4 days; (d) HI, AcOH, 130–140° C, 4 hrs; (e) C$_5$H$_8$O, p-CH$_3$C$_6$H$_4$SO$_3$H-H$_2$O, 0° C 4.5 hrs; (f) AlCl$_3$, CS$_2$, 20 ° C, 22 hrs.

Table 1

The EC$_{50}$ values for E2 and the tested triphenylethylenes in MCF-7:WS8 cells proliferation assays.
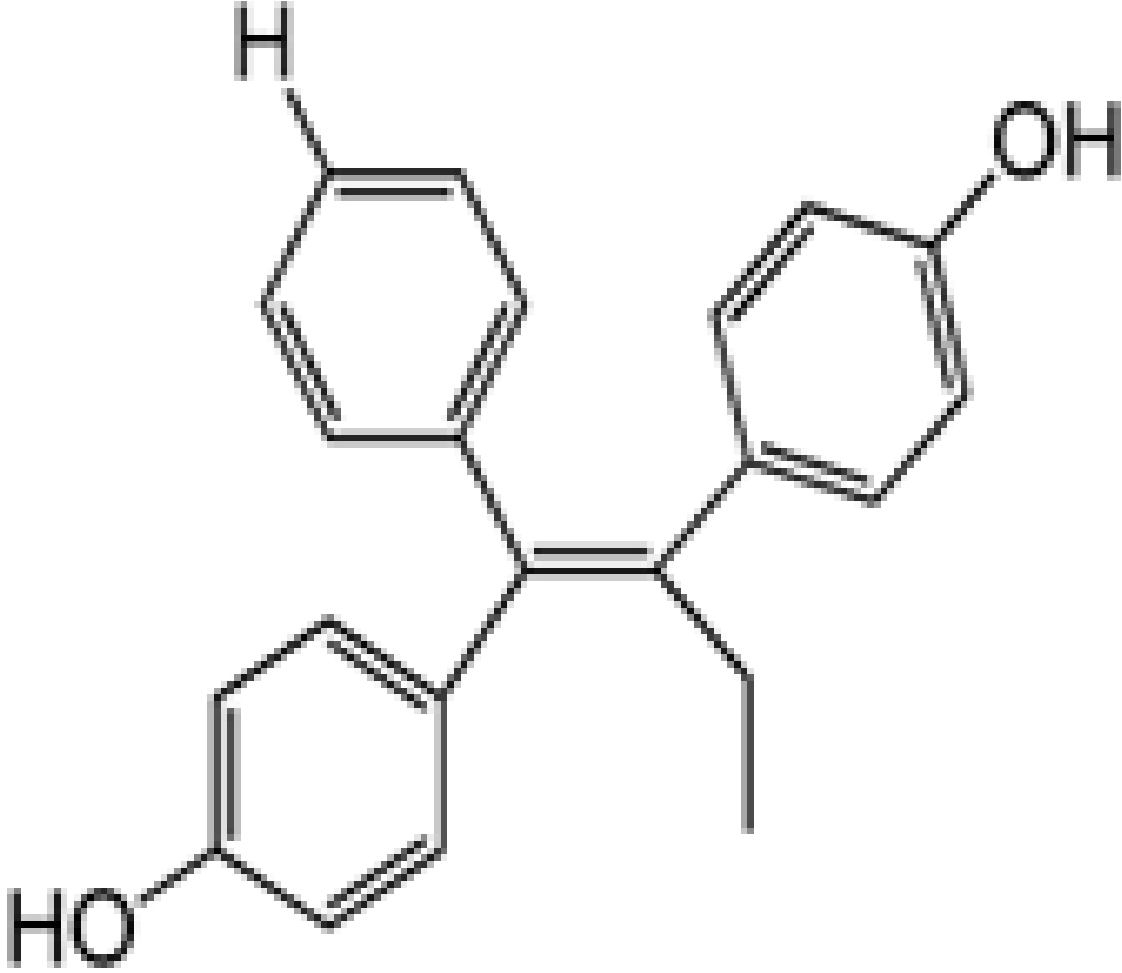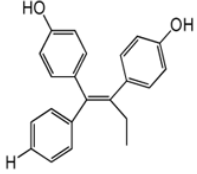
Compound	Structure
E2	
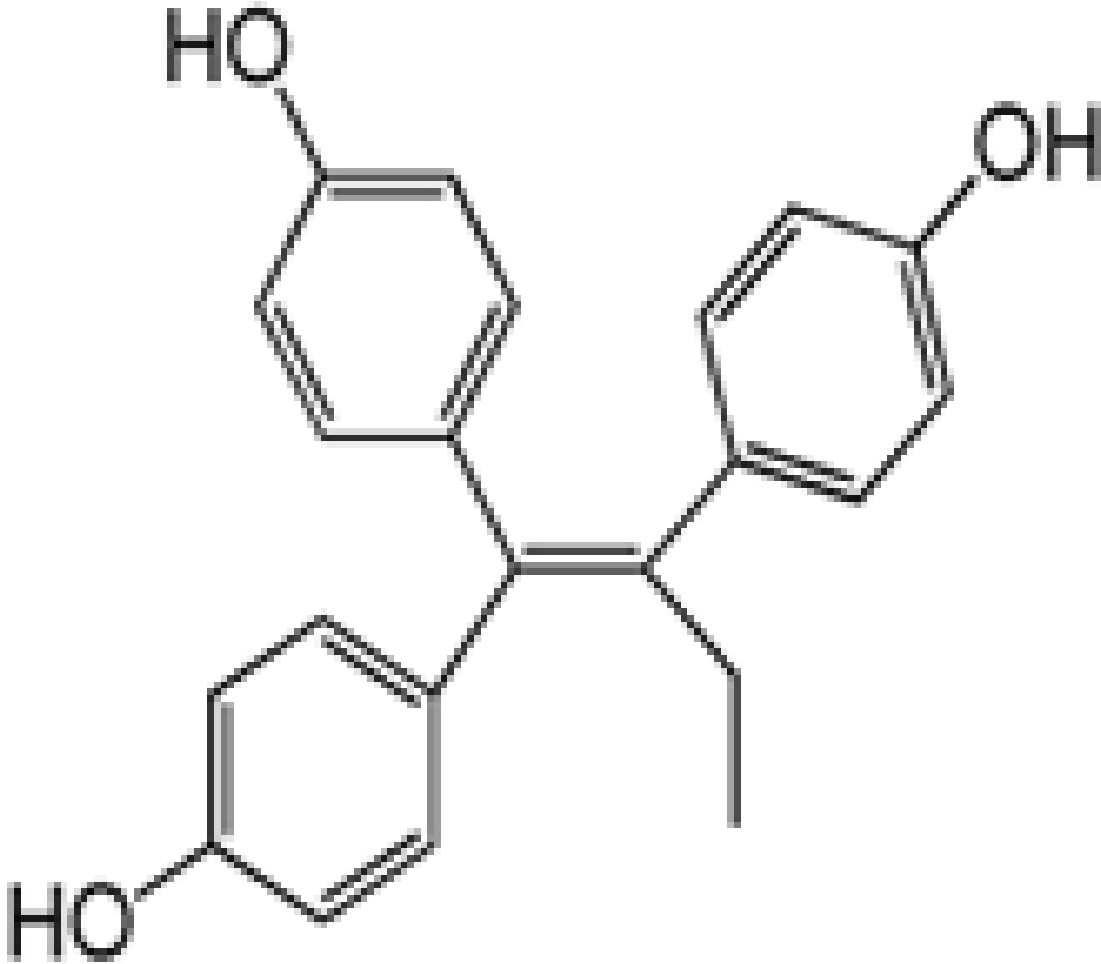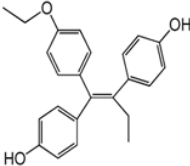
Compound	Structure
15	

Compound	Structure
6	
7	

Compound	Structure
3	
12	